

PNAS



1

2 **Supporting Information for**

3 **Robustness Revisited: On the Neutral Evolution of Centrality and Localization**

4 **Yehonatan Sella and Aviv Bergman**

5 **To whom correspondence should be addressed. E-mail: aviv@einsteinmed.edu**

6 **This PDF file includes:**

- 7 Supporting text
- 8 Figs. S1 to S11
- 9 SI References

Supporting Information Text

Further details on Proposition 1. The limit of \mathbf{p}_t as $t \rightarrow \infty$ can be analyzed using the eigenvectors of B . Since B is symmetric, it is diagonalizable. Thus any vector \mathbf{p}_0 can be decomposed $\mathbf{p}_0 = \sum_i v_i$ as a sum of eigenvectors v_i with eigenvalues λ_i , so that

$$\mathbf{p}_t = \sum_i \frac{\lambda_i^t v_i}{\sum_i \lambda_i^t \mathbf{1}^T v_i}.$$

As t grows large, the terms associated with highest-magnitude eigenvalues dominate. In fact, as t approaches infinity, \mathbf{p}_t will always converge to the same stationary distribution, regardless of the initial distribution \mathbf{p}_0 . This is a consequence of the Perron-Frobenius Theorem applied to B .

Indeed, since B has non-negative entries and is irreducible (meaning its underlying graph is connected, which follows from our assumption that G' is connected), Perron-Frobenius guarantees that the spectral radius $\rho(B)$ is an eigenvalue of B whose eigenspace has dimension 1; moreover, we can choose an eigenvector with eigenvalue $\rho(B)$ all of whose entries are positive, and conversely any eigenvector all of whose entries are positive must have eigenvalue $\rho(B)$. If we normalize by the requirement that the entries add to 1, there is a unique such vector, which we will denote $\tilde{\mathbf{p}}$. We also note that $-\rho(B)$ is not an eigenvalue of B . Indeed, this is again guaranteed by Perron-Frobenius, as a consequence of the fact that B has period 1 (meaning the greatest common divisor of the lengths of loops in the graph underlying B is 1; this follows automatically from the fact that B has positive entries on the diagonal).

Now, we claim that \mathbf{p}_t approaches $\tilde{\mathbf{p}}$ as $t \rightarrow \infty$, no matter the initial distribution \mathbf{p}_0 . The key is that the eigenvector decomposition of \mathbf{p}_0 is bound to include a nonzero component along $\tilde{\mathbf{p}}$. Indeed, if this were not the case, let $r < \rho(B)$ be the highest magnitude of the eigenvalues in the eigen-decomposition of \mathbf{p}_0 . Since eigenvalues with magnitude r (that is, $\lambda = \pm r$) dominate the rest, \mathbf{p}_t will approach an oscillation of the form $v \pm w$, where v and w are eigenvectors with eigenvalues r and $-r$, respectively. So the average of \mathbf{p}_t and \mathbf{p}_{t+1} approaches v , an eigenvector with eigenvalue r . But the \mathbf{p}_t have all positive entries, so by Perron-Frobenius, v must equal $\tilde{\mathbf{p}}$, contradicting $r < \rho(B)$.

In fact, the stationary distribution $\tilde{\mathbf{p}}$ has a simple interpretation. Note that, due to the relationship $B = (1 - \mu)I + \frac{\mu}{N}A$, the matrices A and B have the same eigenvectors. Moreover, though they do not have the same eigenvalues, there is an order-preserving one-to-one correspondence between the eigenvalues of A and B . Thus, the eigenvector $\tilde{\mathbf{p}}$ is also the eigenvector of A with largest eigenvalue. Since A is the adjacency matrix of the graph G' , the vector $\tilde{\mathbf{p}}$ is also known as the eigenvector-centrality of G' . That is, in the stationary distribution, the nodes $v \in V'$ are distributed according to their eigencentrality in the graph G' .

Moreover, we note that, in our model, the stationary distribution does not depend on the mutation rate μ . The rate μ , however, does affect the rate of convergence to the stationary distribution (see also (1)).

Average values of \mathbf{r}_k and \mathbf{l} . We show that the average k th order robustness in the stationary distribution of the mutation-selection evolutionary dynamics is $(\frac{\rho(A)}{N})^k$. Indeed, substituting in the equation $\mathbf{r}_k = \frac{1}{N^k} A^k \mathbf{1}$, we see that $\mathbf{r}_k \cdot \tilde{\mathbf{p}} = \frac{1}{N^k} \mathbf{1}^T A^k \tilde{\mathbf{p}}$ (since A is symmetric). But $\tilde{\mathbf{p}}$ is an eigenvector of A with eigenvalue $\rho(A)$. So $\mathbf{r}_k \cdot \tilde{\mathbf{p}} = (\frac{\rho(A)}{N})^k \mathbf{1}^T \tilde{\mathbf{p}} = (\frac{\rho(A)}{N})^k$.

The average value of \mathbf{l} across the stationary distribution $\tilde{\mathbf{p}}$ is then $\mathbf{l} \cdot \tilde{\mathbf{p}} = \sum_{k=0}^{\infty} \mathbf{r}_k \cdot \tilde{\mathbf{p}} = \sum_{k=0}^{\infty} (\frac{\rho(A)}{N})^k = \frac{1}{1 - \frac{\rho(A)}{N}}$. Note that $\rho(A) \leq N$ always, the case $\rho(A) = N$ occurring only if all states are viable.

Evolution under mutation favors robustness. We first demonstrate the claim that the average values of \mathbf{r}_k and \mathbf{l} increase over the course of evolution under mutation, compared to the uniform distribution. Indeed, the uniform distribution is given by $\frac{1}{|V'|} \mathbf{1}$, and so the average k th-order robustness of the uniform distribution is $\frac{1}{|V'|} \mathbf{1} \cdot \mathbf{r}_k = \frac{1}{|V'| N^k} \mathbf{1}^T A^k \mathbf{1} \leq (\frac{\rho(A)}{N})^k$, where we use the fact that the number $\mathbf{1} \cdot A^k \mathbf{1}$ is bounded by $\rho(A)^k \|\mathbf{1}\|^2 = \rho(A)^k |V'|$. Thus, the average k th-order robustness of the uniform distribution is bounded above by that of $\tilde{\mathbf{p}}$. Equality is only obtained if the uniform distribution $\frac{1}{|V'|} \mathbf{1}$ already equals the stationary distribution $\tilde{\mathbf{p}}$. In this case, all viable nodes have the same number of viable neighbors, and so robustness is uniform across all nodes.

One can recast this calculation as showing that the correlation between the stationary distribution and robustness is positive. Indeed, the difference $\mathbf{r}_k \cdot \tilde{\mathbf{p}} - \frac{1}{|V'|} \mathbf{1} \cdot \mathbf{r}_k$, which we have shown is positive, is precisely $|V'| \text{Cov}(\mathbf{r}_k, \tilde{\mathbf{p}})$.

As a consequence, we also see that the stationary distribution $\tilde{\mathbf{p}}$ positively correlates with \mathbf{l} , since the latter is a positive combination of the \mathbf{r}_k .

While we have shown in general that $\tilde{\mathbf{p}}$ correlates positively with the measures $\mathbf{r}, \mathbf{r}_k, \mathbf{l}$, the precise extent of these correlations varies and depends on the specific structure of the network of viable nodes.

Proof of eigencentality on interval. We claim that the eigencentality of a geometric interval $\{1, \dots, n\}$ is $f(i) = \sin(\frac{i}{n+1}\pi)$ for $1 \leq i \leq n$. Thanks to Perron-Frobenius, since this function is strictly positive, we can prove that it is indeed the stationary distribution by proving that it is an eigenvector of the adjacency matrix A given by $A_{ij} = 1$ if and only if $|i - j| = 1$.

This follows from simple trigonometry. We claim f , restricted to $1 \leq i \leq n$, is an eigenvector of the matrix A with eigenvalue $\lambda = 2\cos(\frac{\pi}{n+1})$. Indeed, the eigenvector equations boil down to

$$f(i-1) + f(i+1) = \sin(\frac{i-1}{n+1}\pi) + \sin(\frac{i+1}{n+1}\pi) = 2\sin(\frac{i}{n+1}\pi)\cos(\frac{\pi}{n+1}) = \lambda f(i)$$

Note that this captures the boundary conditions as well, since $f(i) = 0$ when $i = 0$ or $n+1$.

The above equations are a consequence of the general trigonometric identity

$$\sin(\alpha + \beta) + \sin(\alpha - \beta) = 2\sin(\alpha)\cos(\beta)$$

for any angles α, β (A similar solution for the path graph can be found in (2)).

The formula for the eigencentality of a geometric box can then be obtained by reducing to the case of an interval, by considering product structures of landscapes, discussed below.

Product Structures. We now focus on the special case in which a fitness landscape can be decomposed as a product of fitness landscapes. We formalize this notion below.

Consider two fitness landscapes: the first, a graph $G_1 = (V_1, E_1)$ together with a fitness function $f_1 : V_1 \rightarrow \mathbb{R}^{\geq 0}$; and the second, a graph $G_2 = (V_2, E_2)$ together with a fitness function $f_2 : V_2 \rightarrow \mathbb{R}^{\geq 0}$.

We define the product of these two fitness landscapes to be the following. Its vertex set is $V_1 \times V_2$, and its edges are given by $(v_1, v_2) \sim (v'_1, v_2)$ whenever v_1 is a neighbor of v'_1 in E_1 , and $(v_1, v_2) \sim (v_1, v'_2)$ whenever v_2 is a neighbor of v'_2 in E_2 . In other words, the neighbors of (v_1, v_2) are the results of substituting one of v_1, v_2 with a neighbor, and leaving the other one fixed. Finally, the fitness function on the product is given by $f(v_1, v_2) = f_1(v_1)f_2(v_2)$.

In the special case of holey landscapes, where f_1 and f_2 only take on values of 0 or 1, then this means $f(v_1, v_2) = 1$ whenever both $f_1(v_1) = 1$ and $f_2(v_2) = 1$, and $f(v_1, v_2) = 0$ otherwise.

The structure described above can be generalize to n -dimensions, representing a genetic system composed of n genes whose alleles can mutate among m_i neighboring alleles the i 'th gene can assume. Such a product structure as arising from a genetic system that have no epistatic interaction, in the sense that a fatal mutation in the one gene leads to inviability regardless of the genetic background of the other set of genes.

In the case of holey landscapes, we now demonstrate that the stationary distribution of the product $V_1 \times V_2$ under the setup above is simply the product of the individual stationary distributions on V_1 and V_2 . Let $\tilde{\mathbf{a}}$ and $\tilde{\mathbf{b}}$ denote the stationary distributions on V_1 and V_2 , respectively, and let $\tilde{\mathbf{p}}$ denote the stationary distribution on the product.

To show that $\tilde{p}_{(v_1, v_2)} = \tilde{a}_{v_1}\tilde{b}_{v_2}$, it suffices by Perron-Frobenius to show that $\tilde{a}_{v_1}\tilde{b}_{v_2}$ forms an eigenvector for the adjacency matrix of viable nodes in $V_1 \times V_2$. Indeed, it has eigenvalue $\lambda_1 + \lambda_2$, where λ_1 is the eigenvalue associated to $\tilde{\mathbf{a}}$ in V_1 and λ_2 is the eigenvalue associated to $\tilde{\mathbf{b}}$ in V_2 . This boils down to the following set of equations, for each pair of viable nodes $(v_1, v_2) \in V_1' \times V_2'$:

$$\begin{aligned} & \sum_{v'_1 \sim v_1} \tilde{a}_{v'_1}\tilde{b}_{v_2} + \sum_{v'_2 \sim v_2} \tilde{a}_{v_1}\tilde{b}_{v'_2} \\ &= \tilde{b}_{v_2} \left(\sum_{v'_1 \sim v_1} \tilde{a}_{v'_1} \right) + \tilde{a}_{v_1} \left(\sum_{v'_2 \sim v_2} \tilde{b}_{v'_2} \right) \\ &= \tilde{b}_{v_2} \cdot \lambda_1 \tilde{a}_{v_1} + \tilde{a}_{v_1} \cdot \lambda_2 \tilde{b}_{v_2} = (\lambda_1 + \lambda_2) \tilde{a}_{v_1} \tilde{b}_{v_2} \end{aligned}$$

Thus, given such a product structure $V = V_1 \times V_2$, we may reduce the study of the stationary distribution to the independent components V_1, V_2 .

Localization of eigencentality on an interval. Given our formula above for the eigencentality on an interval $\{1, \dots, n-1\}$, if we normalize eigencentality so it sums to 1, the formula becomes:

$$p(i) = \frac{\sin(\frac{i}{n}\pi)}{\sum_{i=1}^{n-1} \sin(\frac{i}{n}\pi)}$$

The normalized Simpson diversity index of the eigencentality on an interval $\{1, \dots, n-1\}$ is given by $n\mathbf{p} \cdot \mathbf{p} =$

$$n \frac{\sum_{i=1}^{n-1} \sin^2(\frac{i}{n}\pi)}{(\sum_{i=1}^{n-1} \sin(\frac{i}{n}\pi))^2} = \pi \frac{\frac{\pi}{n} \sum_{i=1}^{n-1} \sin^2(\frac{i}{n}\pi)}{(\frac{\pi}{n} \sum_{i=1}^{n-1} \sin(\frac{i}{n}\pi))^2}$$

Both the numerator and denominator above can be understood as Riemann sums, so that in the limit the expression becomes

$$\pi \frac{\int_0^\pi \sin^2(x) dx}{(\int_0^\pi \sin(x) dx)^2} = \pi \frac{\pi/2}{4} = \frac{\pi^2}{8}$$

as claimed.

A similar calculation can be carried out in the case of a geometric square.

Recombination: precise description. Next, we describe sexual reproduction dynamics abstractly. To this end, the graph $G = (V, E)$ must be augmented with the additional structure of a reproduction tensor, which is a function $R : V \times V \times V \rightarrow \mathbb{R}^{\geq 0}$ symmetric with respect to its first two inputs.

The number $R(v_1, v_2, v_3)$ is interpreted as the probability that an offspring with genotype v_3 is produced from a mating of parents with genotypes v_1 and v_2 (discounting mutation). In practice, we only require the information of this tensor on viable nodes; let $R' : V' \times V' \times V' \rightarrow \mathbb{R}^{\geq 0}$ be the restriction of R to V' .

The tensor R will depend on the rate of recombination. To elucidate this, let $0 \leq s \leq 1$ be the recombination rate. Reproduction can be conditioned on the presence or absence of a recombination (crossing-over) event. To represent these two cases, let $R_0 : V \times V \times V \rightarrow \mathbb{R}^{\geq 0}$ be a tensor which describes reproduction without recombination, and $R_1 : V \times V \times V \rightarrow \mathbb{R}^{\geq 0}$ be a tensor which describes reproduction with recombination (here we restrict the process to a single recombination event), so that $R_0(v_1, v_2, v_3)$ (respectively $R_1(v_1, v_2, v_3)$) represents the probability that if parents with genotypes v_1 and v_2 mate without (respectively, with) recombination, they produce an offspring with genotype v_3 .

Then the total reproduction tensor may be written as

$$R_c(v_1, v_2, v_3) = (1 - c)R_0(v_1, v_2, v_3) + cR_1(v_1, v_2, v_3)$$

The subscript indicates the dependence on the parameter c . The tensors R_0 and R_1 are assumed to both be stochastic in the third variable, in the sense that if v_1, v_2 are fixed, and for a given $i = 0, 1$, the probabilities $R_i(v_1, v_2, v_3)$ sum to 1. If the tensor is restricted to V' it will be substochastic in the third variable.

Finally, we define a symmetric quadratic function $Q : \mathbb{R}^{|V'|} \rightarrow \mathbb{R}^{|V'|}$ by

$$Q(\mathbf{x})_v = \sum_{(v_1, v_2) \in V' \times V'} x_{v_1} x_{v_2} R'(v_1, v_2, v)$$

Reproduction dynamics can then be defined simply by $\mathbf{x} \mapsto Q(\mathbf{x})$. If we interpret \mathbf{x} as a population count vector, the dynamics $\mathbf{x} \mapsto Q(\mathbf{x})$ reflect a panmictic population in which every individual mates with every other individual in the population to produce the next generation. That is, we are assuming infinite population and are primarily interested in tracking the population distribution rather than absolute numbers; the resulting dynamics on population distribution captures random mating.

Combined with mutation and selection, the process becomes

$$\mathbf{x} \mapsto B \cdot Q(W\mathbf{x})$$

The standard biological example is that of either haploid or diploid populations, and in which the recombination scheme is given by a set of recombination events. Below we will study both cases of haploid and diploid populations.

In the haploid case, $G = (V, E)$ is the graph of all sequences of length n over a given alphabet \mathcal{A} (a Hamming graph). Here R_0^{hap} represents randomly choosing one of the parents, $R_0^{hap}(\mathbf{v}_1, \mathbf{v}_2, \mathbf{v}_3) = \frac{1}{2}\delta_{\mathbf{v}_1, \mathbf{v}_3} + \frac{1}{2}\delta_{\mathbf{v}_2, \mathbf{v}_3}$ (where $\delta_{\mathbf{u}, \mathbf{v}}$ refers to the Kronecker delta function which equals 1 if and only if $\mathbf{u} = \mathbf{v}$). We focus on a recombination scheme that assumes one crossover event, where the crossover locus is picked at random from among the $n - 1$ possibilities. This is described by the recombination tensor

$$R_1^{hap}(\mathbf{v}_1, \mathbf{v}_2, \mathbf{v}_3) = \frac{\sum_{i=1}^{n-1} R_0^{hap}(X_i(\mathbf{v}_1, \mathbf{v}_2), \mathbf{v}_3)}{n - 1}$$

where $X_i : V \times V \rightarrow V \times V$ is the crossover operation at the i th locus, i.e.

$$X_i((a_1, \dots, a_n), (b_1, \dots, b_n)) = ((a_1, \dots, a_i, b_{i+1}, \dots, b_n), (b_1, \dots, b_i, a_{i+1}, \dots, a_n))$$

As above, we then have $R_r^{hap} = (1 - s)R_0^{hap} + sR_1^{hap}$.

In the diploid case, rather than proceeding by specifying R_0 and R_1 , we relate it to the haploid case. Here we treat the genotype space as $V \times V$, where V represents the underlying haploid space. Then we define:

$$R_s^{dip}((\mathbf{v}_1, \mathbf{v}'_1), (\mathbf{v}_2, \mathbf{v}'_2), (\mathbf{v}_3, \mathbf{v}'_3)) =$$

$$R_s^{hap}(\mathbf{v}_1, \mathbf{v}_2, \mathbf{v}_3) R_s^{hap}(\mathbf{v}'_1, \mathbf{v}'_2, \mathbf{v}'_3)$$

Note that different values of s will be appropriate depending on the biological context. For example, if the graph V represents nucleotide sequences in a small contiguous subset of the total genome, then a small value of s is reasonable, given that a crossover event is unlikely to happen within this small subset of the genome. On the other hand, if V represents the total genome, or if the loci represent genes rather than nucleotide base pairs, then a larger value of s is appropriate.

Diploid landscapes with recessive lethality: the no mutation, no recombination case. In this section we provide a proof for the claim that, in diploid landscapes that are generated using recessive lethality, the dynamics in the case of no mutation and no recombination (that is, only random assortment of gametes) leads to a distribution in which only the double-viable diploids are represented, with viable gamete frequencies proportional to their frequencies in the initial distribution.

To see this, consider a diploid distribution p_{ij}^t , where i and j index the two gametes and the superscript t tracks the generation. We can assume that this distribution is symmetric, i.e. $p_{ij}^t = p_{ji}^t$ since this will be the case after one generation. Let p_i^t denote the total frequency of gamete i , so $p_i^t = \sum_j p_{ij}^t$. Upon recombination, we have the following identities:

If i is viable, then the new frequency of gamete i is given by

$$p_i^{t+1} = \alpha^t \sum_j p_{ij}^t p_j^t = \alpha^t p_i^t$$

where α^t is some fixed re-normalization rate (to get the distribution to add up to 1). On the other hand, if i is inviable, then the new frequency of gamete i is given by

$$p_i^{t+1} = \alpha^t \sum_{j \text{ viable}} p_{ij}^t p_j^t = \alpha^t \beta^t p_i^t$$

where $\beta^t := \sum_{j \text{ viable}} p_j^t$. By summing p_i^{t+1} over all viable gametes, we get that

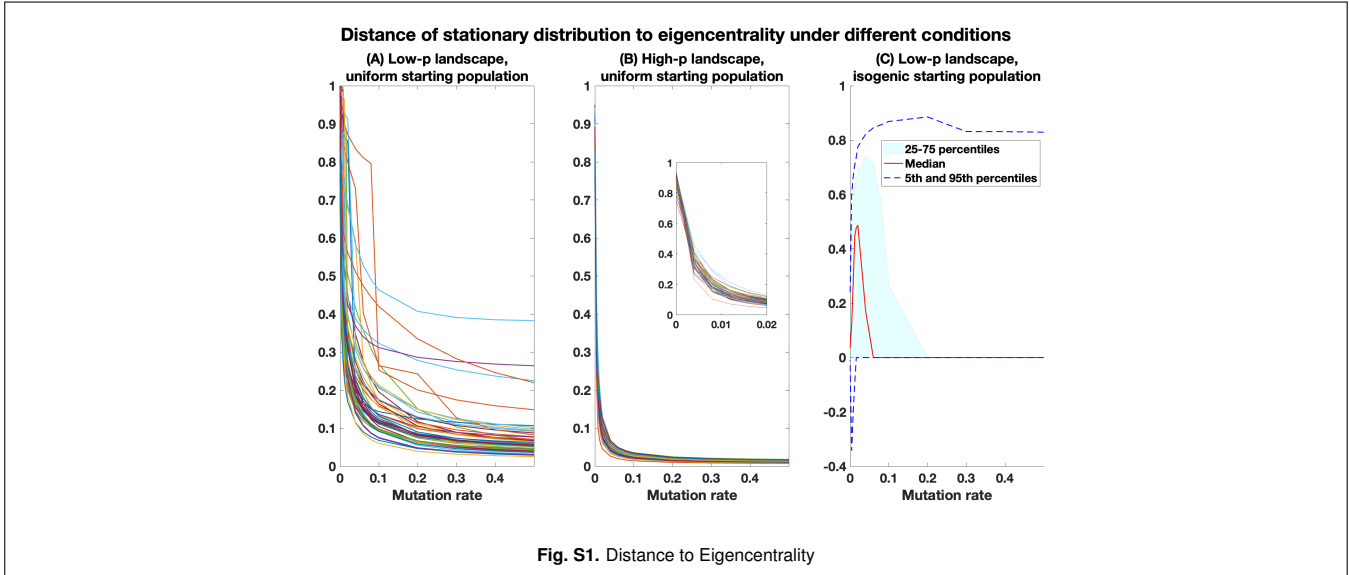
$$\beta^{t+1} = \alpha^t \beta^t$$

Note also that $\alpha^t \geq 1$ for all t by virtue of being a normalization factor, and $\beta^t \leq 1$ for all t by virtue of being a probability. Thus, the sequence of values of β^t is increasing and bounded above, so it must converge. Thus α^t must converge to 1, which implies that in the limit, no inviable diploids are created upon recombination, and so in the limit all gametes are viable. Thus, the distribution of inviable gametes goes to 0, while that of viable gametes is proportional to their initial distributions, as they are always multiplied by the same factor in any given generation.

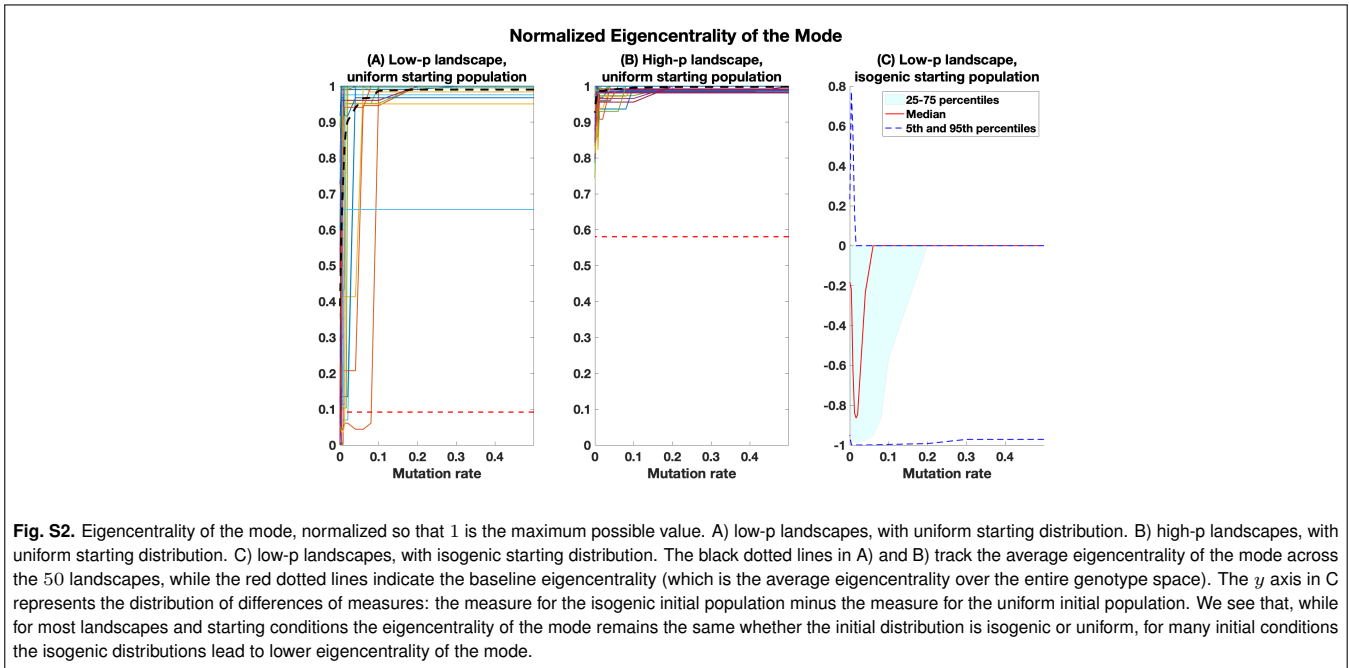
References

1. E Bornberg-Bauer, HS Chan, Modeling evolutionary landscapes: mutational stability, topology, and superfunnels in sequence space. *Proc. Natl. Acad. Sci.* **96**, 10689–10694 (1999).
2. A Böttcher, SM Grudsky, *Spectral properties of banded Toeplitz matrices*. (SIAM), (2005).

174 **An alternative measure of divergence from eigencentality.** An alternative perspective on the interplay between eigencentality
 175 and localization is provided in Figure S1, showing the overall distance between the stationary distribution (measured as total
 176 variation distance between probability densities) and eigencentality. This distance can increase either as a result of heightened
 177 localization or due to a shift in the location of the population's genetic makeup.



178 **Eigencentality of the mode.** To track the shift's in population distribution's locations in the network as the parameters change,
 179 it helps to consider the eigencentality of the mode.



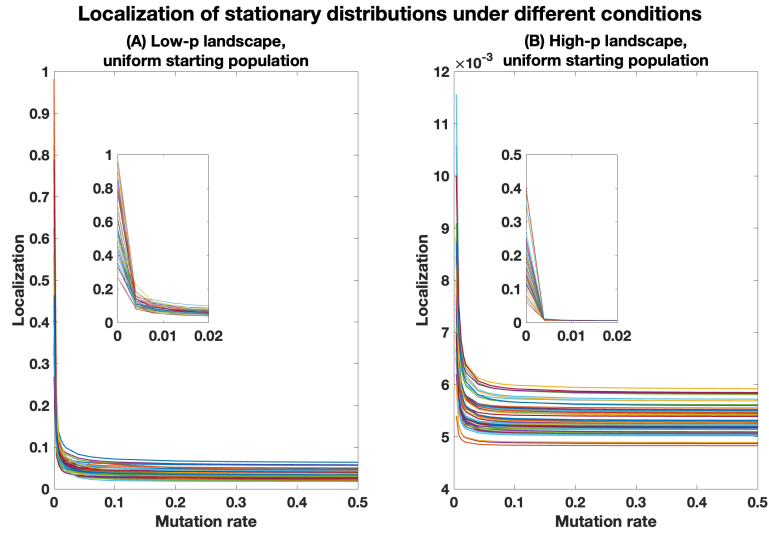


Fig. S3. Dependence of localization on parameters in the haploid regime with mutation and recombination. Here the rate of recombination ($c = 0.05$) is held fixed and the rate of mutation is allowed to vary. In A) and B), the localization is measured for the stationary distributions of 50 randomly generated landscapes (in A with low p and in B with high p) under a uniform starting population.

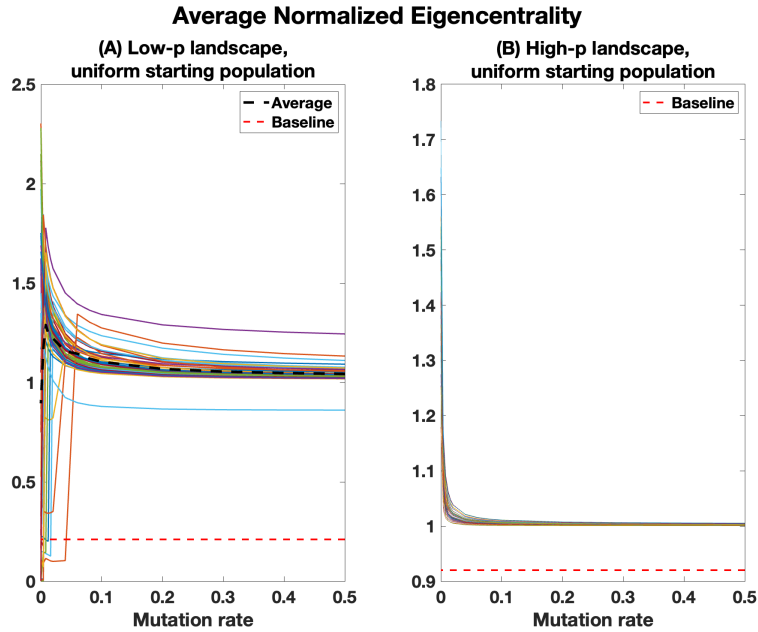


Fig. S4. Divergence between stationary distribution and eigencentality in the presence of recombination. Recombination ($c = 0.05$) is held fixed and the rate of mutation is allowed to vary. In A) and B), the average eigencentality is measured for stationary distributions of 50 randomly generated landscapes (in A, with low p and in B with high p) under a uniform starting population, then normalized by dividing by the corresponding measure of the leading eigenvector distribution itself. A value greater than 1 implies a population distribution which is both located along eigencentral nodes and *localized*.

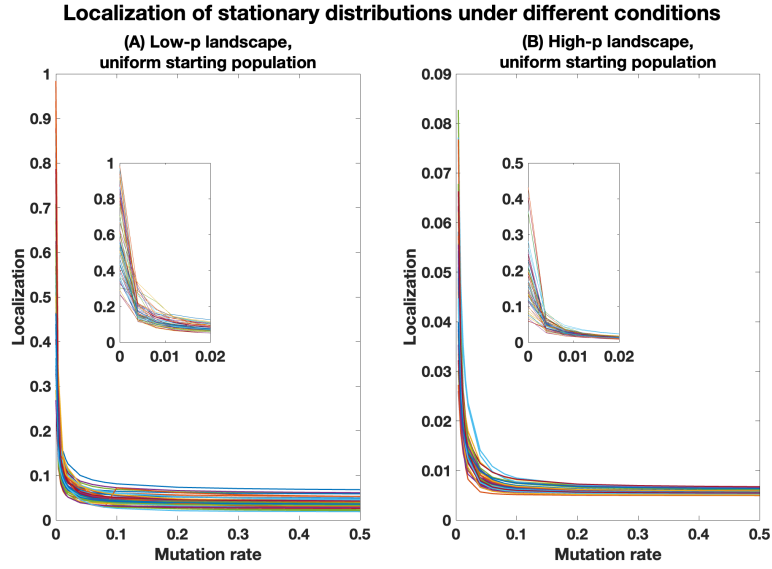


Fig. S5. Dependence of localization on parameters in the haploid regime with mutation and recombination. Here the rate of recombination ($c = 0.5$) is held fixed and the rate of mutation is allowed to vary. In A) and B), the localization is measured for the stationary distributions of 50 randomly generated landscapes (in A with low p and in B with high p) under a uniform starting population.

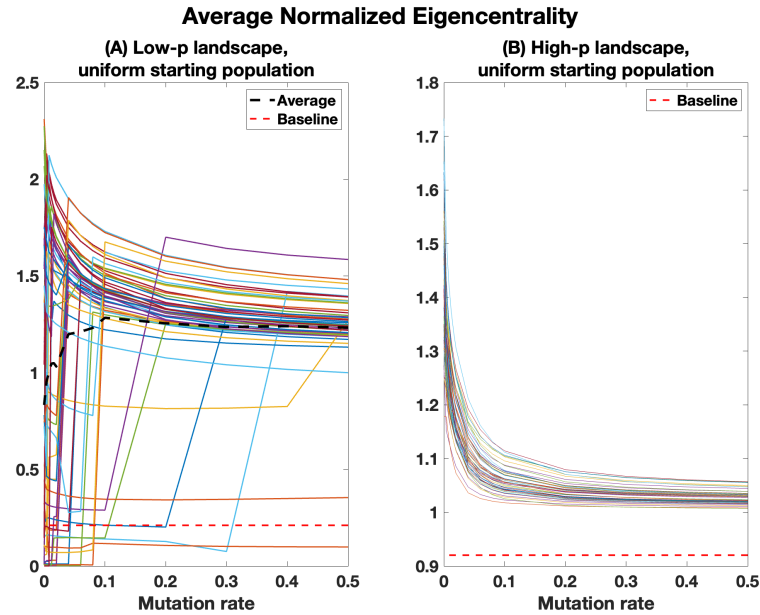


Fig. S6. Divergence between stationary distribution and eigencentality in the presence of recombination. Recombination ($c = 0.5$) is held fixed and the rate of mutation is allowed to vary. In A) and B), the average eigencentality is measured for stationary distributions of 50 randomly generated landscapes (in A, with low p and in B with high p) under a uniform starting population, then normalized by dividing by the corresponding measure of the leading eigenvector distribution itself. A value greater than 1 implies a population distribution which is both located along eigencentral nodes and *localized*.

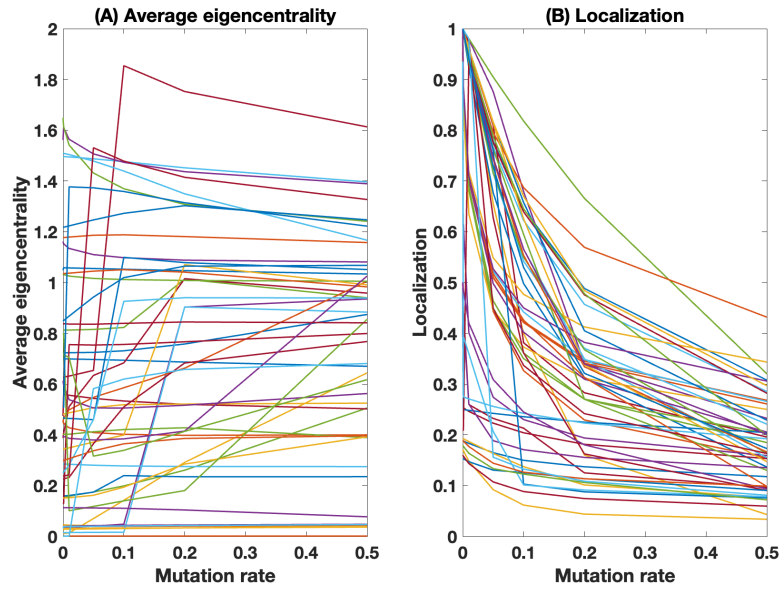


Fig. S7. A) Average Eigencentality (normalized so that 1 is the average eigencentality of the leading eigenvector distribution itself) and B) Localization for 50 random diploid (unstructured) Russian roulette landscapes (recombination rate $c = 0.05$).

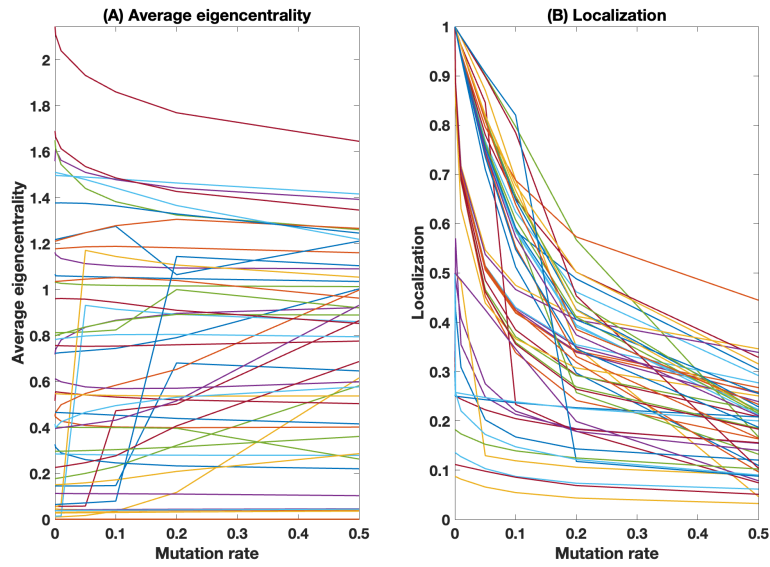


Fig. S8. A) Average Eigencentality (normalized so that 1 is the average eigencentality of the leading eigenvector distribution itself) and B) Localization for 50 random diploid (unstructured) Russian roulette landscapes (recombination rate $c = 0.5$).

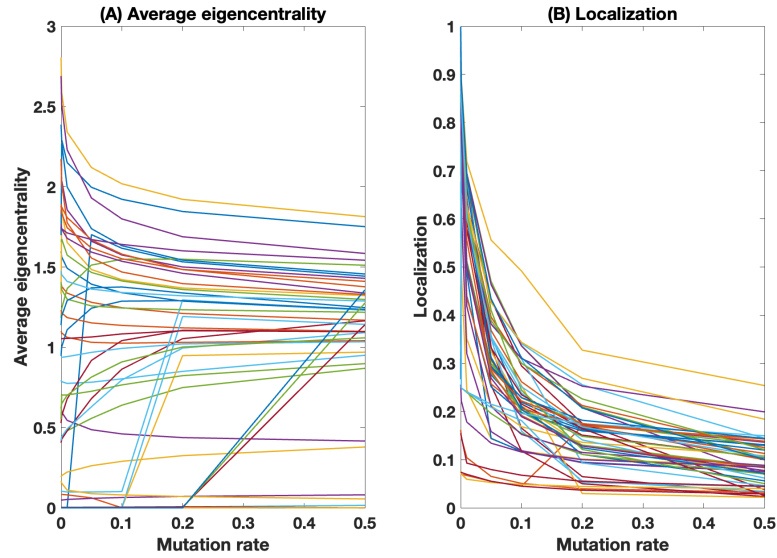


Fig. S9. A second heterozygote paradigm for diploid viability, as introduced in the text, was analyzed. No qualitative differences were observed across a range of values. Here, we present results for $c = 0.1$. A) Average Eigencentality (normalized so that 1 is the average eigencentality of the leading eigenvector distribution itself) and B) Localization for 50 random diploid (unstructured) Russian roulette landscapes.

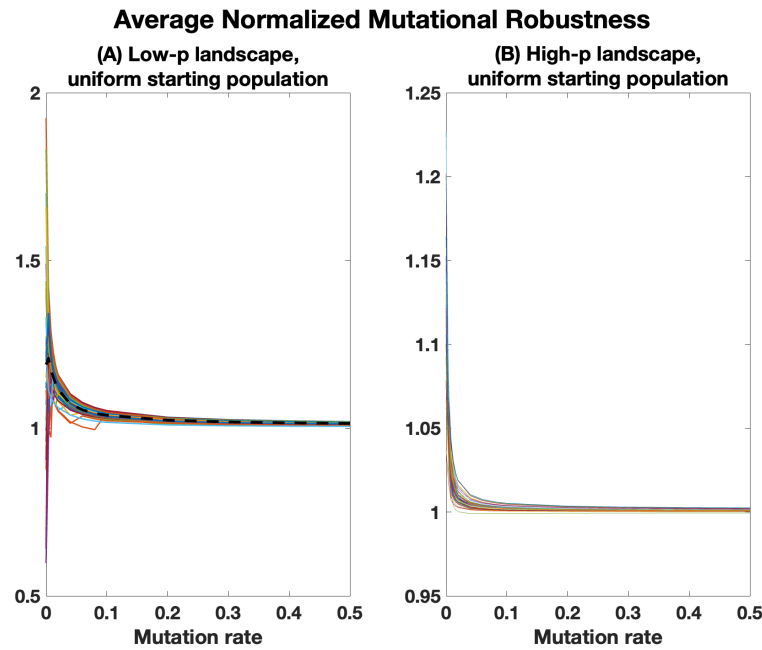


Fig. S10. In A) and B), the average mutational robustness is measured for stationary distributions of 50 randomly generated landscapes (in A, with low $p = 0.2$ and in B with high $p = 0.8$) under a uniform starting population, then normalized by dividing by the corresponding measure of the principal eigenvector distribution itself. We see similar results to those in Figure 5 of the main text, as can be explained by the correlation between mutational robustness and eigencentality. Note that while mutational robustness tends to increase on average with lower mutation rates due to increased localization, several landscapes experience sudden drops in mutational robustness due to the abrupt shifts we note in the main text

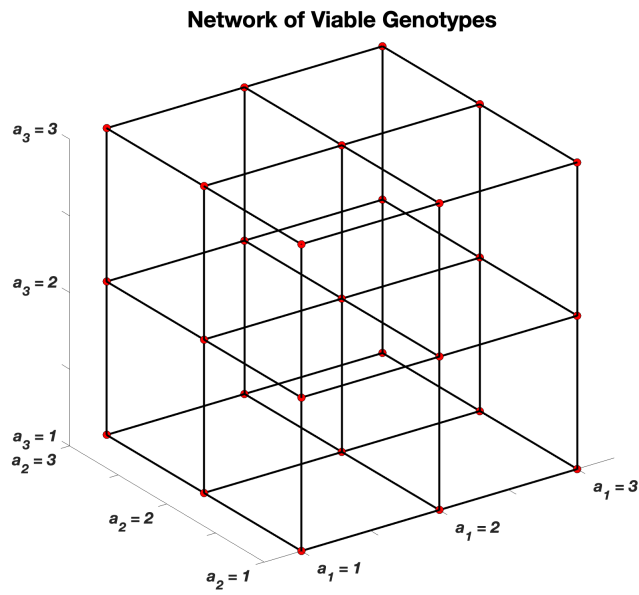


Fig. S11. A graph of the viable nodes in a box landscape in \mathbb{Z}^d , with parameters given by $d = 3$, $n_1 = n_2 = n_3 = 3$. A vertex (a_1, a_2, a_3) is viable if $1 \leq a_i \leq n_i, \forall i$.